Topological dichroism and birefringence of twisted light

Kayn A. Forbes[a,*] and Dale Green[b]

[a]School of Chemistry, University of East Anglia, Norwich Research Park, Norwich, NR4 7TJ, United Kingdom
[b]Physics, Faculty of Science, University of East Anglia, Norwich Research Park, Norwich, NR4 7TJ, United Kingdom

ABSTRACT

Material anisotropy produces differential absorption and birefringence of linearly polarized light; material chirality leads to differential absorption and birefringence of circularly polarized light. Here we highlight how anisotropic media can produce a differential absorption and birefringence which depends on the sign of the topological charge ℓ of a focused optical vortex beam. Manifesting purely through electric-dipole interactions and proportional to the paraxial parameter to first-order, these topological-charge-dependent light-matter interactions are significantly larger than current ℓ-dependent effects which require material chirality and extremely focused light. The interactions described within represent a novel method for probing the local structure of advanced materials and nanoscale light.

Keywords: Structured light, topological charge, dichroism, birefringence, polarization, anisotropic, light-matter interactions, optical angular momentum

1. INTRODUCTION

Light-matter interactions in anisotropic and ordered materials strongly depend on the relative displacement between the driving electromagnetic field and the driven charges and currents. Classic examples of this optical anisotropic behaviour include linear birefringence, utilized in wave plates, for example. Distinct, but also polarization-dependent is optical activity: Chiral materials exhibit polarization-dependent absorption and refraction of circularly polarized light (CPL) through circular dichroism and circular birefringence (optical rotation), respectively. At the microscopic level dichroism involves the absorption of light and birefringence (or refraction) involves the forward Rayleigh (elastic) scattering of light.[1]

Studies and applications to date in the field of optical anisotropy have generally been centred on paraxially propagating light with simple or no structure. A classic example of such a beam would be a well-collimated fundamental Gaussian mode propagating along z and polarized in the x, y plane, i.e. its state of polarization is two-dimensional (2D). In optical activity (chiral) studies, the case is very similar but of course with circular polarization states with helicity $\sigma = \pm 1$ (left-handed $\sigma > 0$, right-handed $\sigma < 0$) generating the required optical chirality that couples to the electric-magnetic dipole response of the material. In the last decade or so the remarkable rise of the field of structured or complex light[2] has occurred, its own genesis being the realization that laser beam photons can carry well-defined orbital angular momentum (OAM) in the direction of propagation[3] of $\ell\hbar$, where $\ell \in \mathbb{Z}$ is the topological charge. Recent studies in chiral light-matter interactions have identified the remarkable optical chirality properties of optical vortex beams (twisted light),[4–15] i.e. structured light which carries OAM. What has been observed is the general fact that light-matter interactions can depend on the sign of the vortex wavefront handedness: left-handed vortex beams $\ell > 0$ interact differently with chiral materials than right-handed vortex beams $\ell < 0$, and this coupling can be completely independent of the 2D polarization state of the beam (i.e. it doesn't require circularly polarized light and $\sigma = 0$). In general, these structured beams needs to be tightly focused to observe the chiral light-matter interactions, and this non-paraxial nature of the electromagnetic fields leads to a general state of polarization which is three-dimensional (3D),[16] i.e. the electromagnetic field has components in the x, y, and z plane. Such topological-charge-dependent light-matter interactions are somewhat limited due to the fact they require higher-order multipolar moments (which are

Further author information: (*Send correspondence to K. A. F.): E-mail: k.forbes@uea.ac.uk

significantly weaker than electric-dipole coupling) and are proportional to the paraxial smallness parameter to second order.

In this work we highlight[17] how focused vortex beams give rise to a ℓ-dependent absorption and refraction in optically anisotropic media (generally achiral). The interactions occur purely through electric-dipole coupling and are proportional to the paraxial parameter to first-order, and thus represent novel light-matter interactions with significantly more broader scope for applications than the current state-of-the-art topological-charge dependent interactions in chiral media.

2. TOPOLOGICAL-CHARGE-DEPENDENT POLARIZATION

The electric field for an arbitrarily polarized z-propagating monochromatic Laguerre-Gaussian (LG) beam in cylindrical coordinates (r, ϕ, z) which includes terms up to first order in the paraxial parameter $1/kw$ (we constrain ourselves to this approximation throughout the manuscript), where k is the wavenumber and w the beam waist, is[18]

$$\mathbf{E} = \big[\alpha\hat{\mathbf{x}} + \beta\hat{\mathbf{y}} + \frac{i}{k}\hat{\mathbf{z}}\big\{\alpha\big(\gamma\cos\phi - \frac{i\ell}{r}\sin\phi\big) + \beta\big(\gamma\sin\phi + \frac{i\ell}{r}\cos\phi\big)\big\}\big]u^{\mathrm{LG}}_{\ell,p}(r,\phi,z), \tag{1}$$

where $\gamma = \frac{\ell}{r} - \frac{2r}{w^2} - \frac{4rL^{\ell+1}_{p-1}}{w^2L^{\ell}_{p}}$; L^{ℓ}_{p} is the generalized Laguerre polynomial; α, β are the Jones vector coefficients: $\alpha^2 + \beta^2 = 1$; $\ell \in \mathbb{Z}$ and $p \in \mathbb{Z}^+$ are the topological charge and radial index, respectively; $u^{\mathrm{LG}}_{\ell,p}(r,\phi,z)$ is the well-known amplitude distribution for LG beams, which includes the all-important azimuthal phase $\mathrm{e}^{i\ell\phi}$. The x and y components of Eq. (1) are the transverse electric field (with respect to the direction of propagation) and account for the 2D polarization state, described using the standard theory of paraxial optics and a 2x2 polarization matrix.[19] The z component is the longitudinal field. The full field, including the non-paraxial longitudinal part, is referred to as 3D polarized and requires a 3x3 polarization matrix to be described.[16]

To elucidate the topological-charge-dependent polarization we concentrate on 2D linearly polarized light in this Section (α and β are real). Note that 2D circularly polarized light ($\beta = i\sigma/\sqrt{2}$) contributes a small in-phase transverse-longitudinal contribution proportional to the helicity σ, but is not topologically dependent, see[17] for more information. The z-polarized, longitudinal field terms in Eq. (1) dependent on γ are $\frac{\pi}{2}$ out of phase with the transverse components due to the i prefactor of the z-components. In calculating the cycle-averaged spin angular momentum density of the field Eq. (1) using $\bar{\mathbf{s}}_{\mathrm{E}} = \mathrm{Im}(\mathbf{E}^* \times \mathbf{E})$ it is easy to show the imaginary longitudinal components lead to a non-zero transverse spin.[20] However, the real longitudinal terms in Eq. (1), which depend on ℓ , are in-phase with the transverse components. Being dependent on ℓ means that this phenomenon of in-phase longitudinal and transverse field components for real α and β is unique to optical vortex modes, and does not manifest in fields where $\ell = 0$, e.g. Gaussian beams or evanescent waves (note this is not the case for 2D polarization with non-zero helicity, see[17]). Most important for us is that the sign of ℓ determines the orientation of the polarization state in xz (see Fig. 1) or yz planes. Analogous behaviour is observed for the magnetic field. This property of ℓ dependent 3D polarization orientation for vortex modes means, in a rather generic sense, that any observable of a light-matter interaction which depends on the polarization vector of the beam (with respect to the material orientation) is modified by the topological structure of generic vortex modes (LG, Bessel, etc.).

3. TOPOLOGICAL DICHROISM

The absorption of light by matter to leading order is described by the interaction Hamiltonian truncated to electric-dipole approximation: $H_{\mathrm{int}} = -\mu_i E_i$ (repeated subscript indices imply Einstein summation convention). The Fermi golden rule tells us the rate of absorption $W_{I\to F}$, is $W_{I\to F} = \frac{2\pi}{\hbar}|\langle F|\ H_{\mathrm{int}}\ |I\rangle|^2\rho(E_{FI})$.[21] The density of states $\rho(E_{FI})$ is specific to the given light-matter system. Using Eq. (1), the amplitude for absorption is:

$$\langle F|\ H_{\mathrm{int}}\ |I\rangle = \big[\alpha\hat{x}_i + \beta\hat{y}_i + \frac{i}{k}\hat{z}_i\big\{\alpha\big(\gamma\cos\phi - \frac{i\ell}{r}\sin\phi\big) + \beta\big(\gamma\sin\phi + \frac{i\ell}{r}\cos\phi\big)\big\}\big]\mu_i u^{\mathrm{LG}}_{\ell,p}, \tag{2}$$

where $\langle\psi_F|\ \mu_i\ |\psi_I\rangle \equiv \mu_i^{FI} \equiv \mu_i$. Retaining terms up to order $\frac{1}{kw}$ (often referred to as the paraxial approximation, though somewhat a misnomer as it includes the non-paraxial longitudinal field) we have for the absorption probability after cycle-averaging over one time period:

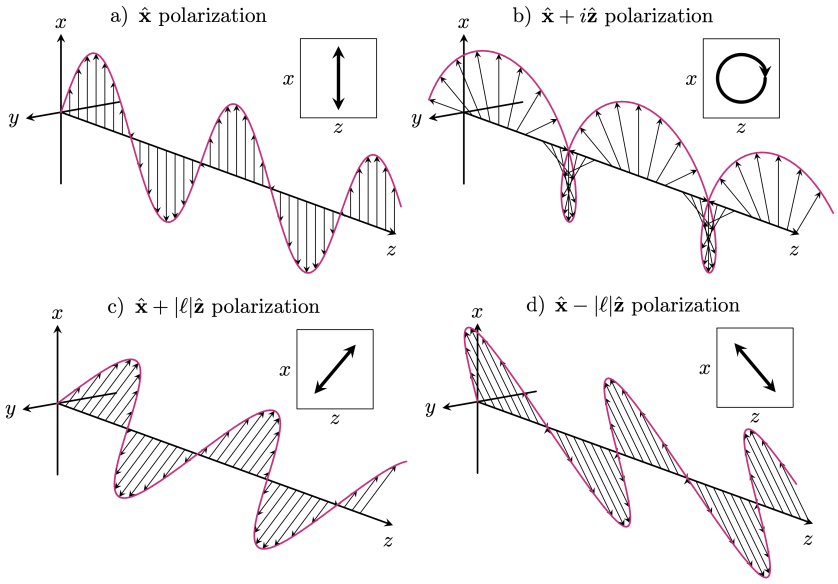

Figure 1. a) 2D x-polarized electric field vector for a z-propagating beam e^{ikz}; b) 2D x-polarized light with $\pi/2$ out-of-phase longitudinal component leading to an elliptical polarization vector in the xz-plane. It is this spinning transverse electric field vector which is responsible for the transverse spin angular momentum of light; c) 2D x-polarized optical vortex light with an in-phase longitudinal field component for positive values of ℓ. The polarization vector is tilted in the positive z-direction in the xz-plane; d) same as c but for negative values of ℓ. In this case the polarization vector is tilted towards the negative z-direction. As is clear from Eq. (1), analogous results would manifest for other 2D states of polarization.

$$|\langle F|\ H_{\rm int}\ |I\rangle|^2 = \mu_i\mu_j\big[|\alpha|^2\hat{x}_i\hat{x}_j + |\beta|^2\hat{y}_i\hat{y}_j + 2\Re\alpha\beta^*\hat{x}_i\hat{y}_j + 2\hat{x}_i\hat{z}_j\frac{1}{k}\big\{(|\alpha|^2\frac{\ell}{r} - \gamma\Im\alpha^*\beta)\sin\phi$$
$$- \frac{\ell}{r}\Re\alpha\beta^*\cos\phi\big\} + 2\hat{y}_i\hat{z}_j\frac{1}{k}\big\{(-\gamma\Im\alpha\beta^* - \frac{\ell}{r}|\beta|^2)\cos\phi + \frac{\ell}{r}\Re\alpha\beta^*\sin\phi\big\}\big]|u^{\rm LG}_{\ell,p}|^2. \tag{3}$$

The first three terms in Eq. (3), zeroth-order with respect to the paraxial parameter $1/kw$, are the well-known contributions to absorption of light under paraxial conditions;[1,21] the remaining terms describe the influence that a focused vortex beam has on absorption. These terms manifest through the interference between the 2D polarized transverse field components and the first-order longitudinal component, and are thus proportional to the paraxial parameter to first order.

There are two important classes of Eq. (3) we can distinguish: whether the input beam is 2D linearly polarized (in which case α and β are real); or whether the input beam is 2D circularly polarized: $\alpha = 1/\sqrt{2}$, $\beta = i\sigma/\sqrt{2}$, where the helicity is $\sigma = \pm 1$, the upper-sign corresponding to left-handed CPL and the bottom right-handed CPL. For the 2D linear case Eq. (3) becomes

$$|\langle F|\ H_{\rm int}\ |I\rangle|^2 = \mu_i\mu_j\big[|\alpha|^2\hat{x}_i\hat{x}_j + |\beta|^2\hat{y}_i\hat{y}_j + 2\Re\alpha\beta^*\hat{x}_i\hat{y}_j + \frac{2\ell}{kr}\big(\hat{x}_i\hat{z}_j\big\{|\alpha|^2\sin\phi - \Re\alpha\beta^*\cos\phi\big\}$$
$$+ \hat{y}_i\hat{z}_j\big\{\Re\alpha\beta^*\sin\phi - |\beta|^2\cos\phi\big\}\big)\big]|u^{\rm LG}_{\ell,p}|^2. \tag{4}$$

The spatial distribution of Eq. (4) and dipole orientation dependence in the focal plane for 2D x-polarized and 2D y-polarized input beams are displayed in Fig. 2 a), e) i) and b), f), j), respectively. The azimuth of the 2D polarization state acts to rotate the spatial distribution of absorption, e.g. compare Fig. 2 e) to Fig. 2 f). More importantly, it is clear that the sign of the topological charge (wavefront handedness) leads to a differential absorption of the light by the material: $W^{\ell}_{I\to F} \neq W^{-\ell}_{I\to F}$. This is analogous to linear and circular dichroism, but the differential effect stems from the topological charge of the vortex beam: topological-charge-dependent

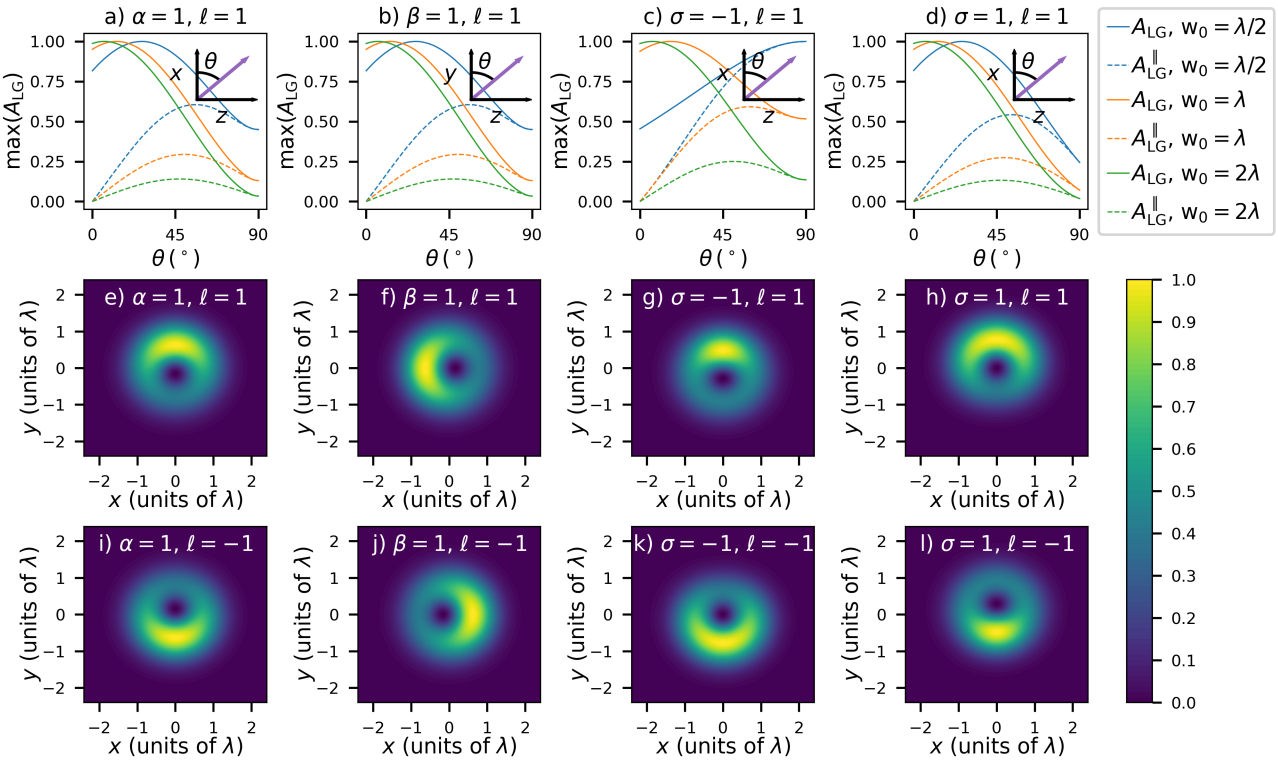

Figure 2. a)–d) Dipole orientation dependence of Eq. (3) for (solid lines) maximum total absorption, $A_{\rm LG}$, individually normalized, (dashed lines) maximum TD contribution, $A_{\rm LG}^{\parallel}$, normalized to the maximum of the solid line of the same color. Insets show dipole orientation with respect to θ and given axes. e)–l) Focal plane spatial distributions of Eq. (3) with $\theta = 45°$, with dipole orientation matching the inset of the corresponding a)–d) of the same column. $p = 0$ in all cases and the magnitude of all dipoles $|\mu_i| = 1$.

dichroism (TD). In the case of 2D CPL Eq. (3) becomes

$$|\langle F|\ H_{\rm int}\ |I\rangle|^2 = \mu_i\mu_j\big[\frac{1}{2}\hat{x}_i\hat{x}_j + \frac{1}{2}\hat{y}_i\hat{y}_j + \hat{x}_i\hat{z}_j\frac{1}{k}\big\{\frac{\ell}{r} - \gamma\sigma\big\}\sin\phi + \hat{y}_i\hat{z}_j\frac{1}{k}\big\{\gamma\sigma - \frac{\ell}{r}\big\}\cos\phi\big]|u_{\ell,p}^{\rm LG}|^2. \tag{5}$$

The spatial distribution of Eq. (5) and dipole orientation dependence in the focal plane for 2D right and left circularly polarized input beams are displayed in Fig. 2 c), g), k) and d), h), l), respectively. There is a clear interplay of terms depending on σ and ℓ. Namely, the case of parallel SAM and OAM (sgnℓ=sgnσ) differs from the anti-parallell SAM and OAM (sgn$\ell\neq$sgnσ): the spatial distribution is more drastically altered by altering the wavefront handedness than the 2D circular polarization handedness, e.g. compare Fig. 2 g) and k) to g) and h). This is because the topological charge influences the 3D polarization state significantly more than the 2D polarization helicity.[17] Furthermore, comparing Fig. 2 c) to Fig. 2 d) highlights how the TD mechanism is significantly larger for the anti-parallel case compared to the parallel case: e.g. for $w_0 = \lambda$ the ratio of the TD contribution to absorption $A_{\rm LG}^{\parallel}$ versus the standard paraxial term is 84%, whereas for the parallel case it is 50%. This behaviour mirrors that which is known for properties (e.g. intensity) of vortex beams due to longitudinal field components.[22]

It is important to appreciate the significant magnitude of the TD mechanism. The intensity of a tightly focused vortex beam, proportional to $\mathbf{E}\cdot\mathbf{E}^*$, consists of the inner product of the dominant 2D transverse fields producing a contribution which is zeroth-order in the paraxial parameter and the inner product of the first-order longitudinal components which yield a contribution that is second-order, i.e. $\propto 1/(kw)^2$. Compared to the 84% ratio for anti-parallel discussed above, the second-order contribution to the intensity proportional to $1/(kw)^2$ is $\approx 10\%$ in optimal conditions for $w_0 = \lambda$ relative to the zeroth-order fields[18] (though readily observed[23]). This highlights the significantly larger TD effect, proportional to first-order in the paraxial parameter $1/(kw)$. TD

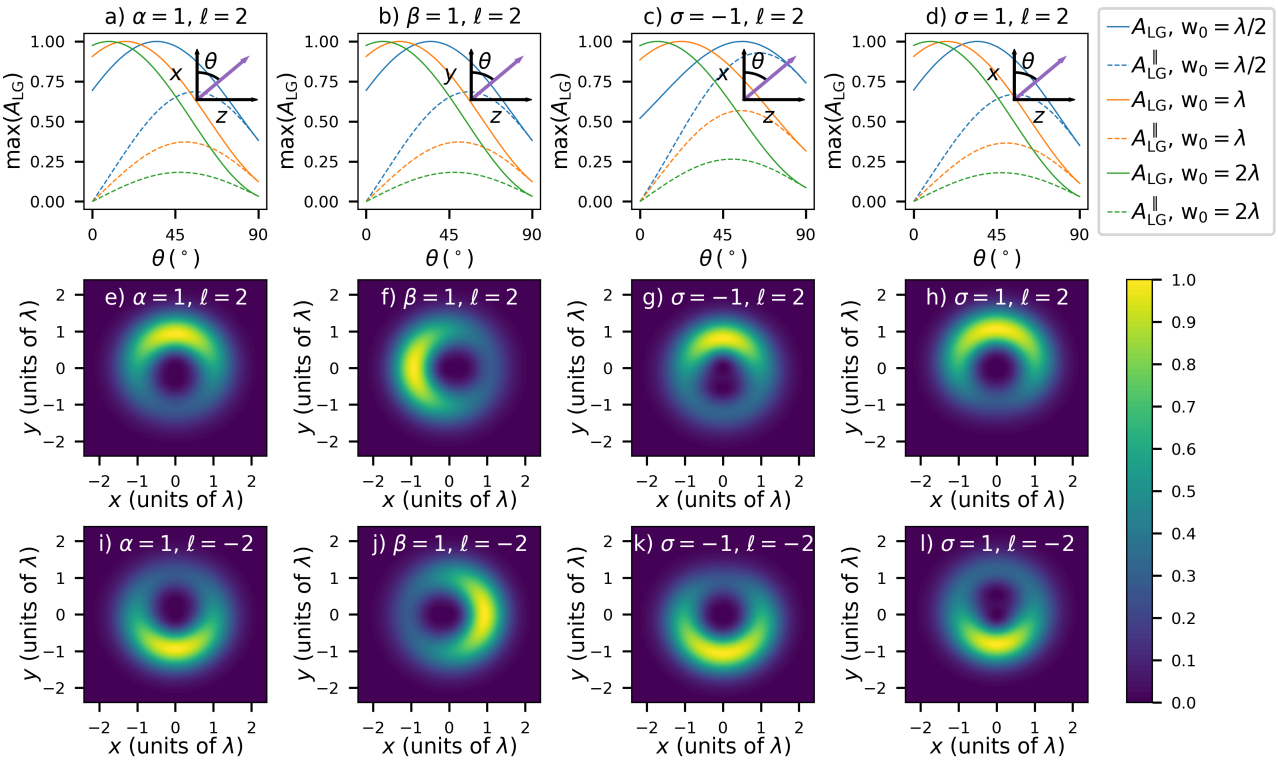

Figure 3. Same as Fig. 2 but for $\ell = 2$.

does not manifest in isotropic media (fluids and gases). This is readily seen by rotational averaging Eq. (3) using the well-known second-rank tensor average: e.g. $\hat{x}_i\hat{z}_j\langle\mu_i\mu_j\rangle = \delta_{ij}\hat{x}_i\hat{z}_j|\mu|^2/3 = 0$.

Laguerre-Gaussian modes are described by both ℓ and the radial index p. We have observed how the sign of ℓ influences TD; here we study the role of the magnitude of ℓ and p. Fig. 3 highlights the linear dependence on the magnitude of ℓ for TD as we see compared to the $\ell = 1$ case of Fig. 2, for $\ell = 2$ the relative contribution of the TD effect increases with increasing ℓ. Figs. 4 and 5 highlights the fact that increasing the radial order p also yields larger relative TD contributions. This is because the magnitude of p controls the $p+1$ concentric rings in the spatial distribution of Laguerre-Gaussian modes. Increasing p increases the transverse gradients of the beam which generate the longitudinal component via $\nabla \cdot \mathbf{E} = 0$. Thus, increasing the transverse gradient increases the magnitude of the first-order longitudinal field component. The TD effect stems from the interference between the transverse and longitudinal field, and so increasing p increases E_z which in turn makes the TD larger for increasing values of p. Note also that increasing p increases TD more significantly relative to increasing ℓ.

The magnitude of TD with respect to the standard dichroic absorption mechanism increases with a tighter focus (smaller w_0); with the value of OAM through a larger ℓ; using the anti-parallel combination of ℓ and σ; increasing the radial order p and manipulating the ratio of $\hat{z}_i\mu_i/\hat{x}_j\mu_j$, which can be achieved by inherent material structure and/or orientation of the absorbing particle/structure.

4. TOPOLOGICAL BIREFRINGENCE

In transparent regions of materials there still manifests differential responses to electromagnetic waves via scattering. Terminology is important here: scattering is generally associated with extinction and a depleted transmission of the input light. However, both linear and circular birefringence at the microscopic level are in fact consequences of elastic scattering in the forward direction, i.e. coherent scattering (as is all refraction).[1,24] To elucidate the qualitative principle of topologically dependent refraction we use the simplest model of a 'dilute' system (low number density of non-polar molecules, neglecting local field effects, etc.). The amplitude for elastic

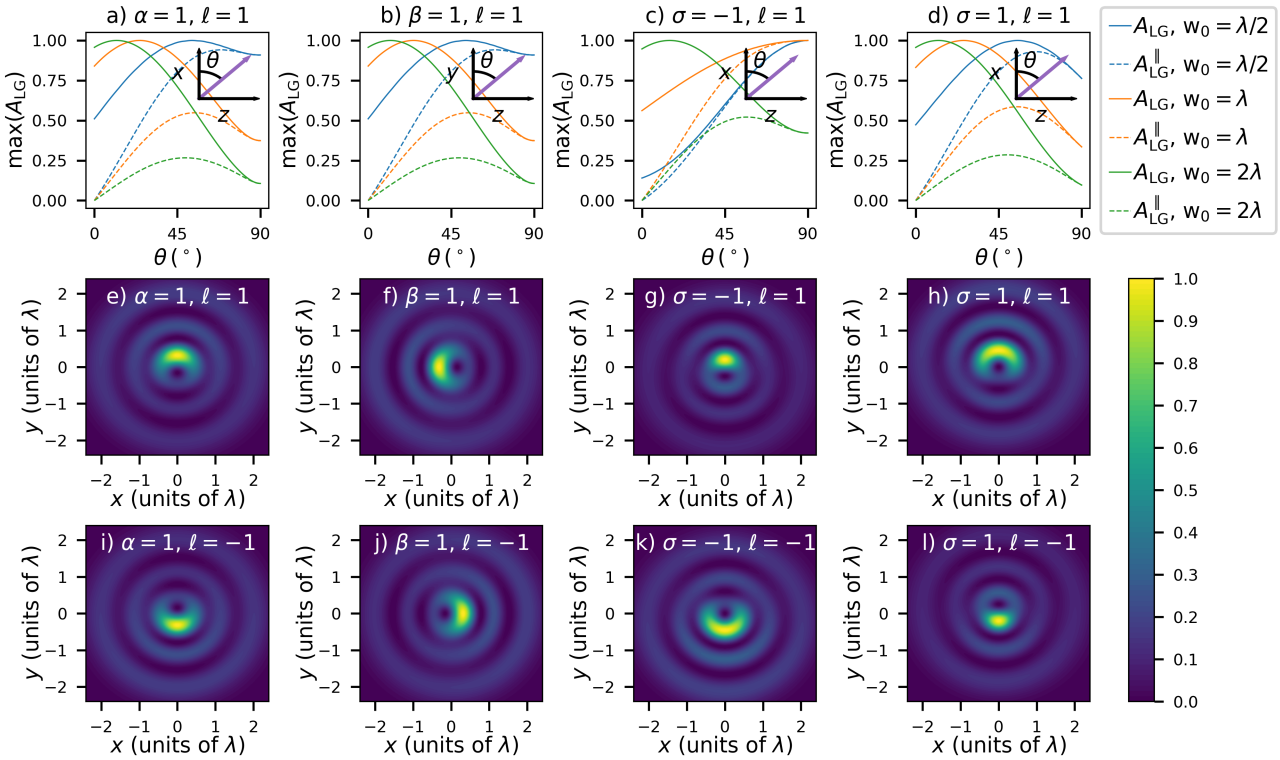

Figure 4. Same as Fig. 2 but for $p = 2$.

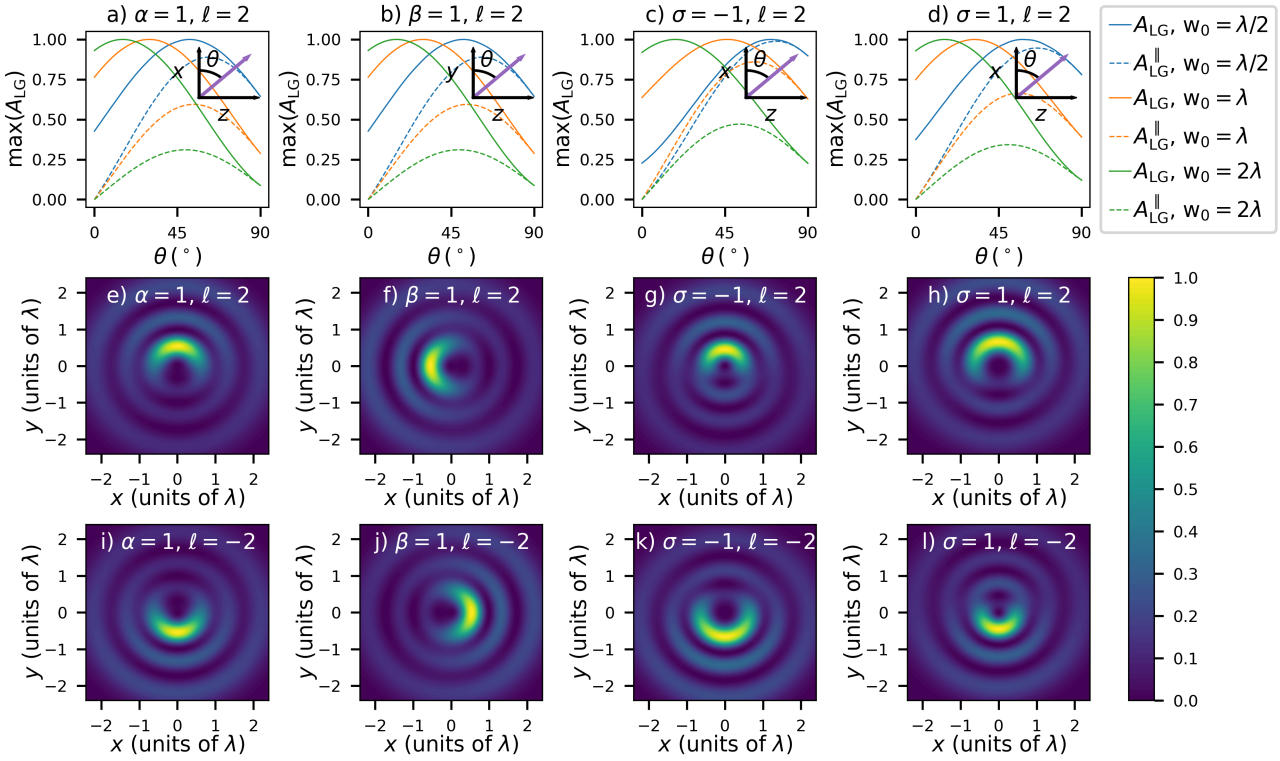

Figure 5. Same as Fig. 2 but for $p = 2$ and $\ell = 2$.

forward scattering, which produces the dynamic Stark shift ΔE and is also responsible for optical trapping,[25] can be related to the refractive index of the molecular medium.[1,26] The forward scattering amplitude of Eq. (1) for a number density N of scattering centres is readily calculated using second-order perturbation theory (see[17] for details):

$$\Delta E = -\frac{NI_{\mathrm{LG}}(r,z)}{2c\epsilon_0}\big[|\alpha|^2\hat{x}_i\hat{x}_j + |\beta|^2\hat{y}_i\hat{y}_j + 2\Re\alpha\beta^*\hat{x}_i\hat{y}_j + 2\hat{x}_i\hat{z}_j\frac{1}{k}\big\{(|\alpha|^2\frac{\ell}{r} - \gamma\Im\alpha^*\beta)\sin\phi - \frac{\ell}{r}\Re\alpha\beta^*\cos\phi\big\} + 2\hat{y}_i\hat{z}_j\frac{1}{k}\big\{(-\gamma\Im\alpha\beta^* - \frac{\ell}{r}|\beta|^2)\cos\phi + \frac{\ell}{r}\Re\alpha\beta^*\sin\phi\big\}\big]\alpha_{ij}(\omega), \tag{6}$$

where $\alpha_{ij}(\omega)$ is the polarizability of the scattering centre and $I_{\mathrm{LG}}(r,z)$ is the intensity of the LG beam. Accounting for energy conservation between the energy density of the field in vacuum and the energy shift experienced by the material, Eq. (6) leads to the following refractive index (see[17]):

$$n = 1 + \frac{N}{2\epsilon_0}\big[|\alpha|^2\hat{x}_i\hat{x}_j + |\beta|^2\hat{y}_i\hat{y}_j + 2\Re\alpha\beta^*\hat{x}_i\hat{y}_j + 2\hat{x}_i\hat{z}_j\frac{1}{k}\big\{(|\alpha|^2\frac{\ell}{r} - \gamma\Im\alpha^*\beta)\sin\phi - \frac{\ell}{r}\Re\alpha\beta^*\cos\phi\big\} + 2\hat{y}_i\hat{z}_j\frac{1}{k}\big\{(-\gamma\Im\alpha\beta^* - \frac{\ell}{r}|\beta|^2)\cos\phi + \frac{\ell}{r}\Re\alpha\beta^*\sin\phi\big\}\big]\alpha_{ij}(\omega). \tag{7}$$

The refractive index Eq. (7) clearly exhibits birefringence with respect to the sign of the topological charge, i.e. $n_\ell \neq n_{-\ell}$. The Stark shift Eq. (6) exhibits the same spatial distribution as TD (see Fig. 2 – 5). Thus, in addition to TD, there also manifests ℓ dependent forward elastic scattering (topological-charge-dependent birefringence) of focused vortex beams at transparent frequencies in oriented materials.

5. DISCUSSION AND CONCLUSION

There has recently been a significant interest in light-matter interactions which are dependent on the wavefront handedness of an optical vortex through the sign of ℓ.[5,9,10,13,27]Studies to date have primarily been concerned with chiral media and the optical chirality of vortex beams, manifesting through the interference of electric dipole coupling with the higher-order magnetic dipole and electric quadrupole interactions. These chiral effects are proportional to the second-order paraxial parameter $1/(kw)^2$ and require multipolar moments which are roughly 1000 times smaller than electric dipole coupling. Nonetheless, such effects have been experimentally observed.[7,11,12,15] Here we have highlighted absorption and forward elastic scattering (refraction) of light by oriented media which depends upon the sign of the topological charge of the input structured optical vortex beam through purely electric dipole interactions (i.e. not requiring chiral materials nor small multipolar couplings) and which are first-order in the paraxial parameter $1/(kw)$. The mechanisms we have discussed in this study should therefore be readily observable, indeed they are of the same order of paraxial parameter as the transverse SAM density of light which is a well-established experimental phenomenon.[28,29]

Compared to existing methods which exploit the handedness associated with the topological charge of vortex beams, techniques based on the phenomena described in this work should be more broadly applicable due to manifesting through purely electric-dipole couplings, thus representing potentially useful methods in the rapidly expanding toolkit of twisted light-matter interactions.[5,13,27,30,31] One-dimensional (1D) and 2D nanostructures are highly suitable structures to exhibit ℓ-dependent absorption (and refraction), with the long-axis oriented parallel to the direction of beam propagation. Examples of these advanced materials which can exhibit TD include liquid crystals, carbon nanotubes and nanoribbons, metamaterials (e.g. hyperbolic plasmonic nanorods[32]), etc. Furthermore, the diverse range of monolayer graphene derivatives and transition metal dichalcogenides,[33] including van der Waals heterostructures,[34,35] also constitute suitable materials to exhibit TD. Clearly, due to its local nature, TD lends itself to nano-optical probing methods, e.g. spatially resolved transmission and 3D Stokes polarimetry techniques. Alternatively, imaging of oriented fluorescent dipole emitters[36] would highlight TD.

The mechanisms we have highlighted have their origins in the fundamental observation that focused optical vortices possess a polarization state orientation which is dependent on the sign of ℓ. As such, the topologically dependent absorption (topological-charge-dependent dichrosim, TD) and forward elastic scattering (topological-charge-dependent birefringence) are generic light-matter interactions for oriented media, and thus open the door for a whole array of specific applications in a wide range of advanced materials.

REFERENCES

[1] Barron, L. D., [*Molecular Light Scattering and Optical Activity*], Cambridge University Press (2009).

[2] Forbes, A., de Oliveira, M., and Dennis, M. R., "Structured light," *Nature Photonics* **15**(4), 253–262 (2021).

[3] Shen, Y., Wang, X., Xie, Z., Min, C., Fu, X., Liu, Q., Gong, M., and Yuan, X., "Optical vortices 30 years on: Oam manipulation from topological charge to multiple singularities," *Light: Science & Applications* **8**(1), 90 (2019).

[4] Forbes, K. A. and Andrews, D. L., "Optical orbital angular momentum: twisted light and chirality," *Optics Letters* **43**(3), 435–438 (2018).

[5] Forbes, K. A. and Andrews, D. L., "Orbital angular momentum of twisted light: chirality and optical activity," *Journal of Physics: Photonics* **3**(2), 022007 (2021).

[6] Forbes, K. A. and Jones, G. A., "Measures of helicity and chirality of optical vortex beams," *Journal of Optics* **23**(11), 115401 (2021).

[7] Ni, J., Liu, S., Wu, D., Lao, Z., Wang, Z., Huang, K., Ji, S., Li, J., Huang, Z., Xiong, Q., et al., "Gigantic vortical differential scattering as a monochromatic probe for multiscale chiral structures," *Proceedings of the National Academy of Sciences* **118**(2), e2020055118 (2021).

[8] Forbes, K. A., "Optical helicity of unpolarized light," *Physical Review A* **105**(2), 023524 (2022).

[9] Forbes, K. A. and Green, D., "Customized optical chirality of vortex structured light through state and degree-of-polarization control," *Physical Review A* **107**(6), 063504 (2023).

[10] Green, D. and Forbes, K. A., "Optical chirality of vortex beams at the nanoscale," *Nanoscale* **15**(2), 540–552 (2023).

[11] Rouxel, J. R., Rösner, B., Karpov, D., Bacellar, C., Mancini, G. F., Zinna, F., Kinschel, D., Cannelli, O., Oppermann, M., Svetina, C., et al., "Hard x-ray helical dichroism of disordered molecular media," *Nature Photonics* **16**(8), 570–574 (2022).

[12] Woźniak, P., De Leon, I., Höflich, K., Leuchs, G., and Banzer, P., "Interaction of light carrying orbital angular momentum with a chiral dipolar scatterer," *Optica* **6**(8), 961–965 (2019).

[13] Porfirev, A., Khonina, S., and Kuchmizhak, A., "Light–matter interaction empowered by orbital angular momentum: Control of matter at the micro-and nanoscale," *Progress in Quantum Electronics* **88**, 100459 (2023).

[14] Forbes, K. A., "Spin angular momentum and optical chirality of poincar\'e vector vortex beams," *arXiv preprint arXiv:2402.05621* (2024).

[15] Jain, A., Bégin, J.-L., Corkum, P., Karimi, E., Brabec, T., and Bhardwaj, R., "Intrinsic dichroism in amorphous and crystalline solids with helical light," *Nature Communications* **15**(1), 1350 (2024).

[16] Alonso, M. A., "Geometric descriptions for the polarization of nonparaxial light: a tutorial," *Advances in Optics and Photonics* **15**(1), 176–235 (2023).

[17] Forbes, K. A. and Green, D., "Topological-charge-dependent dichroism and birefringence of optical vortices," *arXiv preprint arXiv:2401.11992* (2024).

[18] Forbes, K. A., Green, D., and Jones, G. A., "Relevance of longitudinal fields of paraxial optical vortices," *Journal of Optics* **23**(7), 075401 (2021).

[19] Chekhova, M. and Banzer, P., [*Polarization of Light: In Classical, Quantum, and Nonlinear Optics*], Walter de Gruyter GmbH & Co KG (2021).

[20] Bliokh, K. Y. and Nori, F., "Transverse and longitudinal angular momenta of light," *Physics Reports* **592**, 1–38 (2015).

[21] Craig, D. P. and Thirunamachandran, T., [*Molecular quantum electrodynamics: an introduction to radiation-molecule interactions*], Courier Corporation (1998).

[22] Bliokh, K. Y., Rodríguez-Fortuño, F. J., Nori, F., and Zayats, A. V., "Spin–orbit interactions of light," *Nature Photonics* **9**(12), 796–808 (2015).

[23] Iketaki, Y., Watanabe, T., Bokor, N., and Fujii, M., "Investigation of the center intensity of first-and second-order laguerre-gaussian beams with linear and circular polarization," *Optics Letters* **32**(16), 2357–2359 (2007).

[24] Jackson, J. D., [*Classical Electrodynamics*], John Wiley & Sons (1998).

[25] Andrews, D. L. and Bradshaw, D. S., [*Optical nanomanipulation*], Morgan & Claypool Publishers (2016).
[26] Atkins, P. W. and Friedman, R. S., [*Molecular Quantum Mechanics*], Oxford University Press (2011).
[27] Andrews, D. L., "Fundamental symmetry origins in the chiral interactions of optical vortices," *Chirality* **35**(11), 899–913 (2023).
[28] Eismann, J. S., Nicholls, L. H., Roth, D. J., Alonso, M. A., Banzer, P., Rodríguez-Fortuño, F. J., Zayats, A. V., Nori, F., and Bliokh, K. Y., "Transverse spinning of unpolarized light," *Nature Photonics* **15**(2), 156–161 (2021).
[29] Aiello, A., Banzer, P., Neugebauer, M., and Leuchs, G., "From transverse angular momentum to photonic wheels," *Nature Photonics* **9**(12), 789–795 (2015).
[30] Babiker, M., Andrews, D. L., and Lembessis, V. E., "Atoms in complex twisted light," *Journal of Optics* **21**(1), 013001 (2018).
[31] Rosen, G. F. Q., Tamborenea, P. I., and Kuhn, T., "Interplay between optical vortices and condensed matter," *Reviews of Modern Physics* **94**(3), 035003 (2022).
[32] Aigner, A., Dawes, J. M., Maier, S. A., and Ren, H., "Nanophotonics shines light on hyperbolic metamaterials," *Light, Science & Applications* **11** (2022).
[33] Chowdhury, T., Sadler, E. C., and Kempa, T. J., "Progress and prospects in transition-metal dichalcogenide research beyond 2d," *Chemical Reviews* **120**(22), 12563–12591 (2020).
[34] Xiang, R., Inoue, T., Zheng, Y., Kumamoto, A., Qian, Y., Sato, Y., Liu, M., Tang, D., Gokhale, D., Guo, J., et al., "One-dimensional van der waals heterostructures," *Science* **367**(6477), 537–542 (2020).
[35] Guo, J., Xiang, R., Cheng, T., Maruyama, S., and Li, Y., "One-dimensional van der waals heterostructures: A perspective," *ACS Nanoscience Au* **2**(1), 3–11 (2021).
[36] Novotny, L., Beversluis, M., Youngworth, K., and Brown, T., "Longitudinal field modes probed by single molecules," *Physical Review Letters* **86**(23), 5251 (2001).